Mechanics of Solids
Vol. 33, No. 2, pp. 139–149, 1998

Izvestiya AN. MTT
No. 2, pp. 163–174, 1998

ASYMPTOTIC AND NUMERICAL ANALYSES OF HIGH-FREQUENCY FREE VIBRATIONS OF RECTANGULAR PLATES

E. A. Ivanova

(Received 28 September 1995)

Free vibrations of rectangular plates with frequencies belonging to high-frequency spectra are studied. The results predicted by the exact Reissner theory are compared with those predicted by an approximate theory of high-frequency free vibrations which takes into account only functions slowly varying with respect to the spatial coordinates.

It is well known that in solving some dynamical problems of plates, in particular, problems on forced vibrations under the action of impact loadings, one cannot ignore high-frequency vibrations which are associated with the inertia of rotation and the transverse shear deformation. However, so far, high-frequency vibrations have not been studied sufficiently well and their further investigation is of interest from both practical and theoretical viewpoints.

In [1], an asymptotic analysis of equations of free vibrations of plates was carried out in which the inertia of rotation and the transverse shear deformation were taken into account. It was established that for high-frequency vibrations, the solution contains functions rapidly varying with respect to spatial coordinates and penetrating into the entire domain of the plate. The presence of such functions makes the exact equations of the exact Reissner theory practically unsuitable for the numerical analysis of the problems. In [1], an approximate statement of the problem on high-frequency free vibrations of a plate was suggested; only functions that vary slowly with respect to the spatial coordinates are taken into account. The asymptotic accuracy of this statement in $O(h)$ compared with unity in determining natural shapes and $O(h^4)$ in determining natural frequencies (h is the plate thickness). This difference in the accuracy is accounted for by the fact that the leading terms of asymptotic expansions for all natural frequencies coincide and are known, whereas the approximate theory defines the first correcting terms in the asymptotic expansions for the natural frequencies.

Of course, the asymptotic accuracy of a theory is an important characteristic. However, to assess an asymptotic theory from the viewpoint of its practical significance, the actual accuracy of the theory is of importance rather than its asymptotic accuracy. (By the actual accuracy we mean the relative difference of the value of a quantity predicted by the approximate theory and the value of that quantity predicted by the exact theory for the given value of the small parameter.) The present paper deals with the analysis of the actual accuracy of the approximate theory of high-frequency vibrations which was suggested in [1]. In this sense, the current paper is a direct continuation of [1].

The purpose on this research is (i) to determine the area of applicability of the theory suggested in [1] and (ii) to draw attention to problems that may occur in performing computations according to both the approximate theory and the exact Reissner theory.

The investigation is exemplified by problems having exact analytical solution (rectangular plates two opposite sides of which are hinged are considered), which allows us to rule out practically any errors of calculations. Plates of different thicknesses are considered for all types of boundary conditions possible in the Reissner theory.

1. SUMMARY OF THE BASIC EQUATIONS GOVERNING FREE VIBRATIONS OF REISSNER'S PLATE

The equations of motion have the form

$$D\Delta\Delta\Phi + \rho h\ddot{\Phi} - \frac{\rho h^3}{12}\left(1 + \frac{2}{\Gamma(1-\mu)}\right)\Delta\ddot{\Phi} + \frac{\rho^2 h^3}{12G\Gamma}\ddot{\ddot{\Phi}} = 0, \tag{1.1}$$

$$\Delta F - \frac{12\Gamma}{h^2}F - \frac{\rho}{G}\ddot{F} = 0. \tag{1.2}$$

The transverse deflection w, the vector Ψ of rotation angles, the vector $\mathbf{N}$ of transverse forces, and the tensor $\mathbf{M}$ of moments are given by

$$\begin{aligned} w &= -\Phi + \frac{h^2}{6\Gamma(1-\mu)}\Delta\Phi - \frac{\rho h^2}{12G\Gamma}\ddot{\Phi}, \\ \Psi &= \nabla\Phi + \nabla F \times \mathbf{n}, \\ \mathbf{N} &= D\nabla\Delta\Phi - \frac{\rho h^3}{12}\nabla\ddot{\Phi} + Gh\Gamma\nabla F \times \mathbf{n}, \\ \mathbf{M} &= D\left[(1-\mu)\nabla\nabla\Phi + \mu\Delta\Phi\mathbf{a} + \tfrac{1}{2}(1-\mu)(\nabla\nabla F \times \mathbf{n} - \mathbf{n}\nabla\nabla F)\right], \end{aligned} \tag{1.3}$$

where $D = \frac{1}{12}Eh^3/(1-\mu^2)$ is the bending stiffness, $Gh\Gamma$ is the shear stiffness, $G = \frac{1}{2}E/(1+\mu)$, Γ is the transverse shear coefficient, E is Young's modulus, μ is Poisson's ratio, ρ is the mass density, h is the plate thickness, $\mathbf{n}$ is the unit normal to the plate plane, $\mathbf{a} = \mathbf{E} - \mathbf{nn}$, and $\mathbf{E}$ is the identity tensor.

The Reissner theory allows one to satisfy three conditions at the contour and, hence, eight different types of boundary conditions are possible. They are listed below.

1. Clamping:

$$w\big|_c = 0, \quad \Psi_\nu\big|_c = 0, \quad \Psi_\tau\big|_c = 0. \tag{1.4}$$

2. Sliding fixing:

$$N_\nu\big|_c = 0, \quad \Psi_\nu\big|_c = 0, \quad \Psi_\tau\big|_c = 0. \tag{1.5}$$

3. Reinforced free edge:

$$N_\nu\big|_c = 0, \quad M_\nu\big|_c = 0, \quad \Psi_\tau\big|_c = 0. \tag{1.6}$$

4. Free edge:

$$N_\nu\big|_c = 0, \quad M_\nu\big|_c = 0, \quad M_\tau\big|_c = 0. \tag{1.7}$$

5. Weakened clamping:

$$w\big|_c = 0, \quad \Psi_\nu\big|_c = 0, \quad M_\tau\big|_c = 0. \tag{1.8}$$

6. Weakened sliding fixing:

$$N_\nu\big|_c = 0, \quad \Psi_\nu\big|_c = 0, \quad M_\tau\big|_c = 0. \tag{1.9}$$

7. Constrained hinged support:

$$w\big|_c = 0, \quad M_\nu\big|_c = 0, \quad \Psi_\tau\big|_c = 0. \tag{1.10}$$

8. Free hinged support:

$$w\big|_c = 0, \quad M_\nu\big|_c = 0, \quad M_\tau\big|_c = 0. \tag{1.11}$$

Here Ψ_ν and Ψ_τ are the angels of rotation of the tangent and normal to the contour, respectively, N_ν is the shearing force, M_ν is the bending moment, and M_τ is the torsional moment.

In the Reissner plate theory, there are three spectra of natural frequencies for which the asymptotic estimates

$$\begin{aligned} \omega_i^{(1)} &= h\omega_{1i}^{(1)} + h^2\omega_{2i}^{(1)} + \cdots, \\ \omega_i^{(2)} &= \sqrt{12G\Gamma/(\rho h^2)} + \omega_{0i}^{(2)} + \cdots, \\ \omega_i^{(3)} &= \sqrt{12G\Gamma/(\rho h^2)} + \omega_{0i}^{(3)} + \cdots, \end{aligned} \tag{1.12}$$

are valid. The first spectrum is a low-frequency bending spectrum (it also exists in the Kirchhoff theory), and the second and third spectra are high-frequency shear and bending spectra which occur due to taking into account the inertia of rotation and the transverse shear deformation, respectively (these spectra are absent from the Kirchhoff theory).

In what follows, we discuss only vibrations with frequencies belonging to the second and third spectra of (1.12). By "high" frequencies we mean frequencies that are high in the asymptotic sense, i.e., belong to high-frequency spectra. The discussion of low-frequency vibrations with large mode numbers is beyond the scope of the present paper.

2. STATEMENT OF THE PROBLEM ON HIGH-FREQUENCY VIBRATIONS OF REISSNER'S PLATE WITHOUT REGARD TO RAPIDLY VARYING FUNCTIONS

Consider the basic equations of the approximate theory of high-frequency vibrations suggested in [1]. The equations of motion have the form

$$\Delta F - \frac{12\Gamma}{h^2}F - \frac{\rho}{G}\ddot{F} = 0, \tag{2.1}$$

$$\left(\Gamma + \frac{2}{1-\mu}\right)\Delta\Phi - \frac{12\Gamma}{h^2}\Phi - \frac{\rho}{G}\ddot{\Phi} = 0. \tag{2.2}$$

Since this theory has the fourth order in spatial coordinates, it allows one to satisfy only two conditions at the contour and, hence, there are four types of boundary conditions in this theory. We specify below these boundary conditions and indicate the corresponding boundary conditions of the exact Reissner theory.

1. Clamping, Eq. (1.4), sliding fixing, Eq. (1.5), and reinforced free edge, Eq. (1.6):

$$\left[\frac{\partial\Phi}{\partial\nu} + \frac{\partial F}{\partial\tau}\right]_c = 0, \quad \left[\frac{\partial\Phi}{\partial\tau} - \frac{\partial F}{\partial\nu}\right]_c = 0. \tag{2.3}$$

2. Free edge, Eq. (1.7), weakened clamping, Eq. (1.8), and weakened sliding fixing, Eq. (1.9):

$$\left[\frac{\partial\Phi}{\partial\nu} + \frac{\partial F}{\partial\tau}\right]_c = 0, \quad D(1-\mu)\left[\frac{\partial^2\Phi}{\partial\nu\partial\tau} + \left(\frac{1}{R}\frac{\partial F}{\partial\nu} + \frac{\partial^2 F}{\partial\tau^2}\right)\right]_c - \left[\frac{\rho h^3}{12}\ddot{F} + Gh\Gamma F\right]_c = 0. \tag{2.4}$$

3. Constrained hinged support, Eq. (1.10):

$$D(1-\mu)\left[\frac{\partial^2 F}{\partial\nu\partial\tau} - \left(\frac{1}{R}\frac{\partial\Phi}{\partial\nu} + \frac{\partial^2\Phi}{\partial\tau^2}\right)\right]_c + \left[\frac{\rho h^3}{12}\ddot{\Phi} + Gh\Gamma\Phi\right]_c = 0, \quad \left[\frac{\partial\Phi}{\partial\tau} - \frac{\partial F}{\partial\nu}\right]_c = 0. \tag{2.5}$$

4. Free hinged support, Eq. (1.11):

$$\begin{aligned} &D(1-\mu)\left[\frac{\partial^2 F}{\partial\nu\partial\tau} - \left(\frac{1}{R}\frac{\partial\Phi}{\partial\nu} + \frac{\partial^2\Phi}{\partial\tau^2}\right)\right]_c + \left[\frac{\rho h^3}{12}\ddot{\Phi} + Gh\Gamma\Phi\right]_c = 0, \\ &D(1-\mu)\left[\frac{\partial^2\Phi}{\partial\nu\partial\tau} + \left(\frac{1}{R}\frac{\partial F}{\partial\nu} + \frac{\partial^2 F}{\partial\tau^2}\right)\right]_c - \left[\frac{\rho h^3}{12}\ddot{F} + Gh\Gamma F\right]_c = 0. \end{aligned} \tag{2.6}$$

Here ν, τ is a local coordinate system introduced on the plate contour, and $R(\tau)$ is the radius of curvature of the contour at a given point.

The vector Ψ of rotation angles and the vector $\mathbf{N}$ of transverse forces are expressed via the potentials F and Φ as

$$\Psi = \nabla\Phi + \nabla F \times \mathbf{n}, \quad \mathbf{N} = Gh\Gamma(\nabla\Phi + \nabla F \times \mathbf{n}). \tag{2.7}$$

The deflection and the tensor of moments are asymptotically small compared with the vector of rotation angles and the vector of transverse forces ($w \sim h^2\Psi$, $\mathbf{M} \sim h^2\mathbf{N}$) and are not determined within the framework of the approximate theory in question.

3. FREE VIBRATIONS OF A RECTANGULAR PLATE HINGED AT TWO OPPOSITE SIDES

Consider a plate occupying a domain $-a \le x \le a$, $-b \le y \le b$. The constrained hinged support conditions (1.10) are assumed to be satisfied at the sides $y = \pm b$, and the boundary conditions at the sides $x = \pm a$ can be arbitrary. We study vibrations symmetric with respect to the axes $x = 0$ and $y = 0$. The natural shapes satisfying the differential equations (1.1) and (1.2) and the boundary conditions (1.10) at $y = \pm b$ have the form

$$\Phi_n(x,y) = \left[C_{1n}\cos(\lambda_{1n}x) + C_{2n}\cos(\lambda_{2n}x)\right]\cos(\mu_n y), \quad F_n(x,y) = C_{3n}\sin(\delta_n x)\sin(\mu_n y), \tag{3.1}$$

where

$$\lambda_{1n} = \sqrt{A_n - B_n}, \quad \lambda_{2n} = \sqrt{A_n + B_n}, \quad \mu_n = \frac{(2n-1)\pi}{2b}, \quad \delta_n = \sqrt{\frac{\rho\omega_n^2}{G} - \frac{12\Gamma}{h^2} - \mu_n^2},$$

$$A_n = \left[1 + \tfrac{1}{2}\Gamma(1-\mu)\right]\frac{\rho\omega_n^2}{2G\Gamma} - \mu_n^2, \quad B_n = \sqrt{\frac{\rho h}{D} + \left[1 - \tfrac{1}{2}\Gamma(1-\mu)\right]\frac{\rho\omega_n^2}{2G\Gamma}}.$$

By satisfying the boundary conditions at $x = \pm a$, one reduces the problem to solving a system of homogeneous algebraic equations for the coefficients C_{1n}, C_{2n}, and C_{3n}. By equating the determinant of this system to zero, one obtains an equation for determining natural frequencies. We considered all types of boundary conditions possible in the Reissner theory and obtained the frequency equations for each of them.

Let us discuss the solution of the problem according to the approximate theory of high-frequency free vibrations [1]. It can be readily shown that the natural shapes satisfying the differential equations (2.1) and (2.2) and the constrained hinged support conditions (2.5) at $y = \pm b$ have the form

$$\Phi_n(x,y) = C_{1n}\cos(\lambda_{1n}x)\cos(\mu_n y), \quad F_n(x,y) = C_{3n}\sin(\delta_n x)\sin(\mu_n y), \tag{3.2}$$

where

$$\lambda_{1n} = \sqrt{\frac{\rho}{G}\frac{\omega_{0n}}{\Gamma + 2/(1-\mu)} - \mu_n^2}, \quad \delta_n = \sqrt{\frac{\rho}{G}\omega_{0n} - \mu_n^2}, \quad \omega_{0n} = \omega_n^2 - \frac{12G\Gamma}{\rho h^2}.$$

The asymptotic analysis shows that the frequency equations and the natural shapes predicted by the asymptotic theory in question follow from the exact frequency equations and the exact natural shapes within an $O(h)$ asymptotic error for all types of boundary conditions (by exact frequency equations and exact vibrational shapes we mean those obtained by the Reissner theory).

4. FREE VIBRATIONS OF A RECTANGULAR PLATE. COMPARATIVE ANALYSIS OF NUMERICAL RESULTS OBTAINED BY THE EXACT REISSNER THEORY AND BY THE APPROXIMATE THEORY OF HIGH-FREQUENCY FREE VIBRATIONS

The numerical analysis was carried out for the problem discussed in Section 3. Computations were performed for plates of dimensions $a = b = 1$ m and thicknesses $h = 0.1$ m and $h = 0.04$ m with the elastic constants $E = 2.1 \times 10^{11}$ Pa, $\mu = 0.25$, $\Gamma = 5/6$, and $\rho = 7.951 \times 10^3$ kg/m^3.

The key results can be summarized as follows.

1. The first 10 natural frequencies of high-frequency spectra are found. The calculations were performed by the Reissner theory and by the approximate theory for all types of boundary conditions possible in the Reissner theory ($h = 0.1$ m and $h = 0.04$ m).

2. The actual errors of the approximate theory are found. The calculations were performed for all types of boundary conditions and the plate thicknesses 0.1 m and 0.04 m.

3. For the case in which the free edge conditions were imposed at the sides $x = \pm a$, more detailed investigation was carried out. The first 10 natural frequencies for plates of thickness 0.2 m, 0.3 m, 0.4 m, and 0.5 m and the corresponding actual errors are calculated. For plates of thickness 0.1 m, the first 33 natural frequencies and the corresponding actual errors are found.

4. The natural shapes corresponding to the first 10 natural frequencies are determined. The calculations were performed by the exact and approximate theories for all types of boundary conditions and the plate thickness 0.1 m. In the case of the free edge conditions, the natural shapes are found for the plate of thickness 0.04 m as well.

5. For the natural shapes in calculation of which the approximate theory leads to the largest errors, the graphs of the rotation angles Ψ_x and Φ_y versus the coordinate x are constructed.

Let us proceed to a detailed discussion of the results obtained.

Tables 1–4 present the first five natural frequencies of high-frequency spectra predicted by the Reissner theory and the approximate theory for plates of thickness 0.1 m and all types of boundary conditions possible in the Reissner theory. The tables also show the relative errors δ of the approximate theory and the relative errors Δ due to the approximation of the natural frequencies by its leading asymptotic term:

$$\delta = \frac{|\omega_R - \omega|}{\omega_R} \times 100\%, \quad \Delta = \frac{\omega_R - \sqrt{12G\Gamma/(\rho h^2)}}{\omega_R} \times 100\%.$$

Here ω_R is the frequency predicted by the Reissner theory and ω is the frequency predicted by the approximate theory. The error Δ is of interest for the following reason. A characteristic feature of high-frequency spectra is the coincidence of the leading asymptotic terms of all natural frequencies, with the relative deviation of the frequencies from the leading term of their asymptotic expansions being small (which is confirmed by the data for Δ presented in Tables 1–4). In this connection, the fact that the errors δ are small says nothing by itself. The errors δ must be much smaller than Δ rather than merely small. It is in this case that one can state that the approximate theory suggested in [1] possesses a sufficiently high actual accuracy.

The results presented in Tables 1–4 allow us to conclude that the actual accuracy of calculation of natural frequencies by the approximate theory is quite high for all types of boundary conditions and $h = 0.1$ m. (Therefore, presenting results for thinner plates makes no sense.) The actual accuracy for natural frequencies depends on the type of boundary conditions at $x = \pm a$; the largest errors occur for the case of the free edge conditions. That is why this type of boundary conditions is chosen for more detailed investigation. Tables 5 and 6 present results for higher natural frequencies (6th through 25th) for $h = 0.1$ m and the results for the first five natural frequencies for thicker plates ($h = 0.2$, 0.3, 0.4, and 0.5 m).

Let us point out some general features characteristic of high-frequency spectra S and the approximation of these spectra by the approximate theory.

1. The frequencies of the bending spectrum b are higher than those of the shear spectrum s. (Calculation show that for all types of boundary conditions at $x = \pm a$, only two frequencies of the first ten belong to the bending spectrum.)

2. The accuracy for the frequencies belonging to the bending spectrum is, as a rule, less than that for the frequencies belonging to the shear spectrum. This is quite natural, since in the approximate theory, the equation responsible for the shear vibrations is exact, whereas the equation responsible for the bending vibrations is approximate.

3. While the approximate theories when applied to low-frequency vibrations yield higher values for the natural frequencies compared with the exact ones, this is not the case for high-frequency vibrations.

4. For high-frequency vibrations, no monotonic increase in the relative error with the mode number is observed either. Of course, lower frequencies are, on the average, predicted more accurately than higher frequencies. However, for high-frequency vibrations, the situation in which a frequency with a larger mode number is predicted more accurately than many frequencies with smaller mode numbers is usual.

5. It was established that in calculation of natural frequencies with large mode numbers, the approximate theory predicts most frequencies with quite high accuracy; however, there are few frequencies for which the errors are considerable. For example, in the case of the free edge conditions at the sides $x = \pm a$ for $h = 0.1$ m (see Table 5), only three frequencies—14th, 22nd, and 25th—of the first 25 are predicted with insufficiently high accuracy. Currently, we cannot explain with certainty the fact that some frequencies are calculated with low accuracy. Perhaps, the approximate theory is unsuitable for calculating so high frequencies (then, however, it is not clear why all other frequencies are predicted with quite high accuracy). It seems more probable (and the author is inclined to think so) that the 14th, 22nd, and 25th frequencies do not belong to high-frequency spectra but are very high frequencies of the low-frequency spectrum. Then these frequencies, predicted by the approximate theory, in fact correspond to other, higher frequencies of high-frequency spectra.

6. When calculating natural frequencies for thicker plates (see Table 6), a similar phenomenon is observed, just as was the case in the calculation of frequencies with large mode numbers. While most frequencies are predicted rather well, there are few frequencies for which the errors are too large. The cause of this phenomenon is either in the fact that the approximate theory fails for so large plate thicknesses or in the fact that frequencies of the low-frequency spectrum enter the frequency range under consideration. The author believes that the latter is more probable.

Let us briefly dwell on the results of calculation of natural shapes. We carried out the investigation of the accuracy provided by the approximate theory for natural shapes as follows. For all types of boundary conditions, analytical expressions for the potentials $F(x, y)$ and $\Phi(x, y)$ were obtained according to the exact and approximate theories. Then the natural shapes represented by $F(x, y)$ were compared with those represented by $\Phi(x, y)$. As a result, it was

Table 1

No	ω_R	Δ	ω	δ	S
			Clamping		
1	102911.492	0.123	102911.492	0	s
2	103293.758	0.493	103291.188	0.002488	b
3	103919.750	1.092	103919.750	0	s
4	103980.492	1.150	103980.523	0.000030	s
5	104602.156	1.737	104598.508	0.003488	s
			Sliding fixing		
1	102911.492	0.123	102911.492	0	s
2	103290.617	0.490	103291.188	0.000553	b
3	103919.750	1.092	103919.750	0	s
4	103979.859	1.149	103980.523	0.000639	s
5	104598.352	1.734	104598.508	0.000149	s
			Reinforced free edge		
1	102911.492	0.123	102911.492	0	s
2	103223.344	0.521	103291.188	0.031122	b
3	103919.750	1.092	103919.750	0	s
4	103987.688	1.157	103980.523	0.006890	s
5	104646.703	1.779	104598.508	0.046050	s

Table 2

No	ω_R	Δ	ω	δ	S
			Free edge		
1	102911.492	0.123	102911.492	0	s
2	103230.133	0.431	103227.633	0.002420	b
3	103465.258	1.658	103416.852	0.046780	s
4	103919.750	1.104	103919.750	0	s
5	104544.000	1.712	104420.227	0.118390	s
			Weakened clamping		
1	102911.492	0.123	102911.492	0	s
2	103226.945	0.430	103227.633	0.000660	b
3	103416.859	0.615	103416.852	0.000007	s
4	103919.750	1.104	103919.750	0	s
5	104420.227	1.591	104420.227	0	s
			Weakened sliding fixing		
1	102911.492	0.123	102911.492	0	s
2	103226.945	0.430	103227.633	0.000660	b
3	103416.852	0.615	103416.852	0	s
4	103919.750	1.104	103919.750	0	s
5	104420.227	1.591	104420.227	0	s

Table 3

No	ω_R	Δ	ω	δ	S
			Constrained hinged support		
1	102911.492	0.123	102911.492	0	s
2	103416.852	0.611	103416.852	0	b
3	103665.891	0.850	103668.602	0	s
4	103919.750	1.092	103919.750	0	s
5	104420.227	1.566	104420.227	0	s

Table 4

No	ω_R	Δ	ω	δ	S
			Free hinged support		
1	102911.492	0.123	102911.492	0	s
2	103038.063	0.246	103038.063	0	b
3	103294.836	0.494	103291.359	0.003366	s
4	103790.852	0.970	103792.211	0.001309	s
5	103816.555	0.994	103804.844	0.011280	s

Table 5

No	ω_R	Δ	ω	δ	S
6	104923.086	2.080	104918.320	0.004540	s
7	105106.242	2.209	104980.414	0.119710	b
8	105907.477	3.038	105907.477	0	s
9	106005.859	3.134	105907.469	0.092810	s
10	106500.523	3.615	106398.602	0.095690	s
11	106658.109	3.768	106704.406	0.043	b
12	107363.789	4.455	107374.117	0.010	s
13	107963.133	5.038	107858.570	0.097	s
14	108184.828	5.254	113338.445	4.764	b
15	108320.070	5.385	108400.984	0.075	b
16	108821.000	5.873	108821.000	0	s
17	109040.453	6.086	110071.414	0.945	b
18	109368.594	6.405	109299.039	0.064	s
19	110018.156	7.037	110248.891	0.210	s
20	110697.523	7.698	110720.766	0.021	s
21	110762.344	7.761	110720.766	0.038	s
22	110879.008	7.875	108340.852	2.289	s
23	112076.461	9.040	111658.523	0.373	s
24	112351.570	9.308	113510.813	1.032	s
25	112368.102	9.324	118069.609	5.074	b

Table 6

No	ω_R	Δ	ω	δ	S
			$h = 0.2$		
1	51645.371	0.12	51645.371	0	s
2	52225.282	0.43	52272.488	0.09	b
3	52390.117	1.65	52645.168	0.49	s
4	53448.188	1.10	55536.676	3.91	s
5	53626.332	1.71	53626.332	0	s
			$h = 0.3$		
1	34639.914	1.10	34639.914	0	s
2	35504.234	2.63	35568.137	0.38	b
3	35764.320	4.39	36113.617	0.98	s
4	37329.172	8.95	40211.961	7.72	s
5	37529.492	9.54	37529.492	0	s
			$h = 0.4$		
1	26198.504	1.95	26198.504	0	s
2	27304.615	6.26	27414.049	0.40	b
3	27623.482	7.50	28118.164	1.79	s
4	29526.547	14.91	33218.063	12.50	s
5	29914.891	16.42	29914.891	0	b
			$h = 0.5$		
1	21181.492	3.04	21181.492	0	s
2	22643.225	10.15	22667.689	0.11	b
3	23961.994	16.56	23514.361	1.87	s
4	25635.811	24.71	25635.811	0	s
5	27135.977	31.86	20644.014	9.24	b

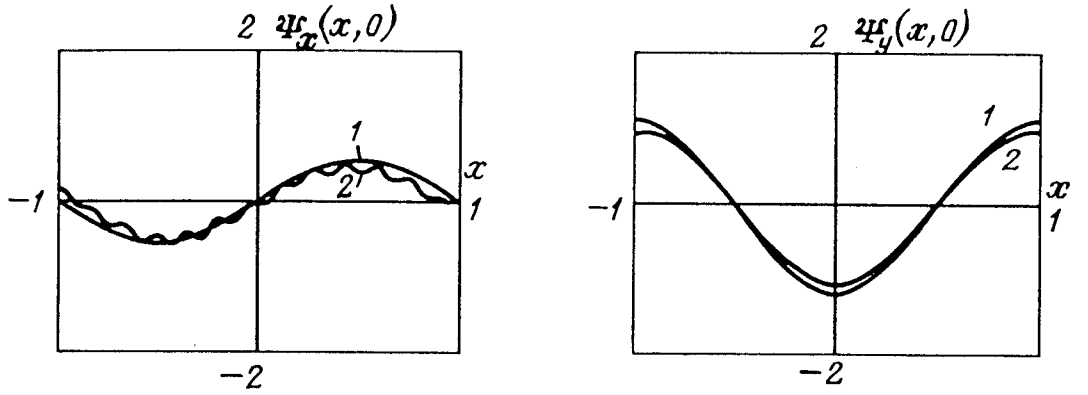

Fig. 1

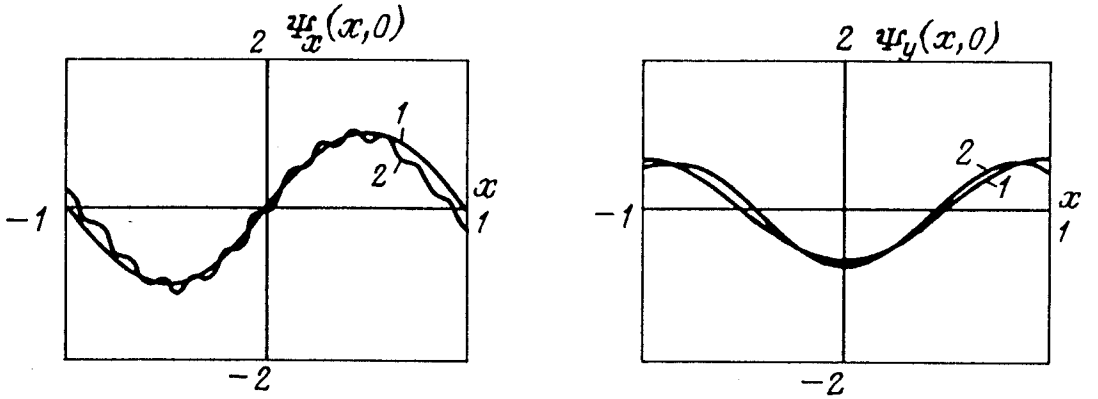

Fig. 2

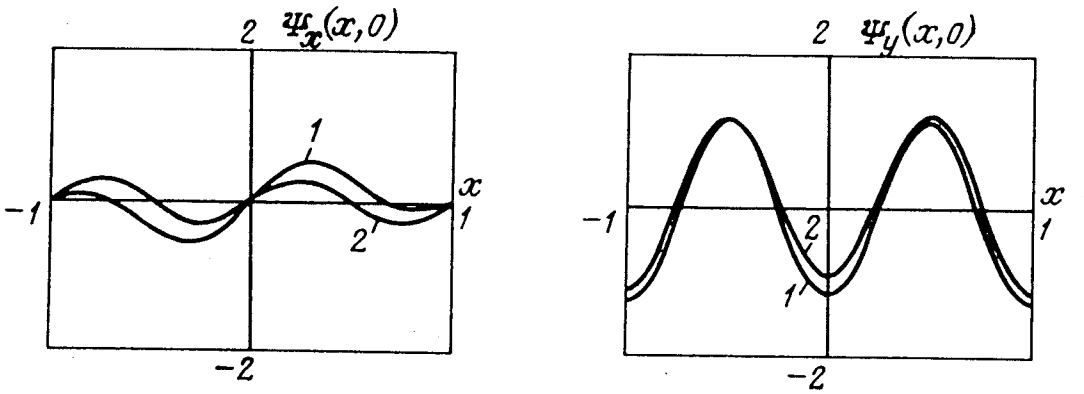

Fig. 3

established that most of natural shapes predicted by the approximate theory virtually coincide with those predicted by the exact Reissner theory. The errors turned out to be noticeable only in the case of the free edge conditions at $x = \pm a$. Therefore, the subsequent discussion pertains just to this type of boundary conditions ($h = 0.1$ m). Figures 1–6 present the first 10 natural vibrational shapes for the plate free at the sides $x = \pm a$, except for the zero natural shapes and the natural shapes whose representations in the exact and approximate theories completely coincide. Figures 1–6 depict the 3rd, 5th, 6th, 7th, 9th, and 10th natural shapes, respectively. The figures show the graphs of the rotation angles Ψ_x and Ψ_y versus the coordinate x (the dependences on the y-coordinate are not of interest, since they completely coincide with those predicted by the exact theory). One can see that the natural shapes predicted by the approximate

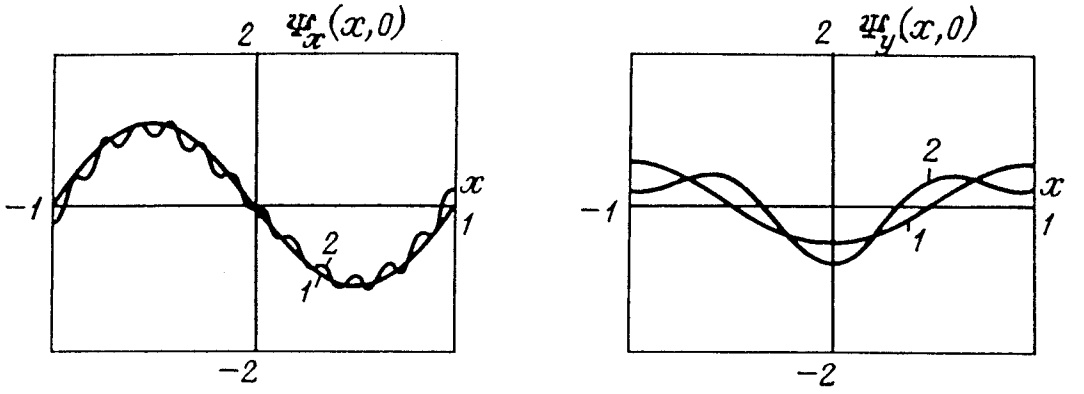

Fig. 4

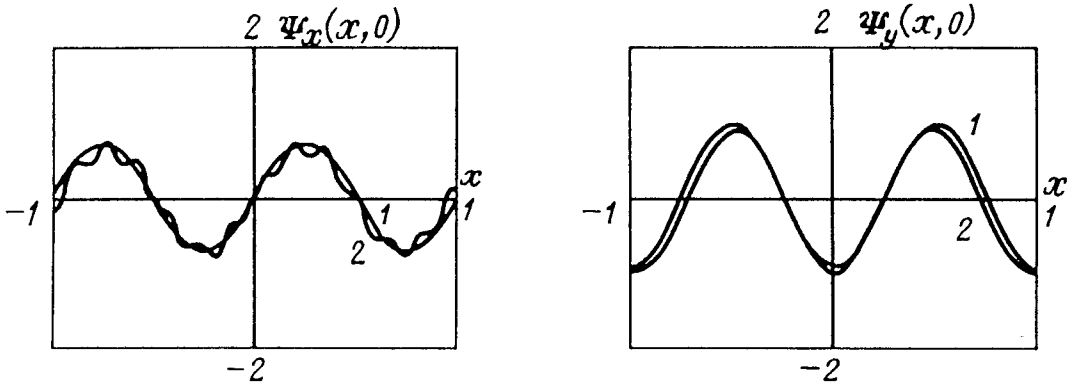

Fig. 5

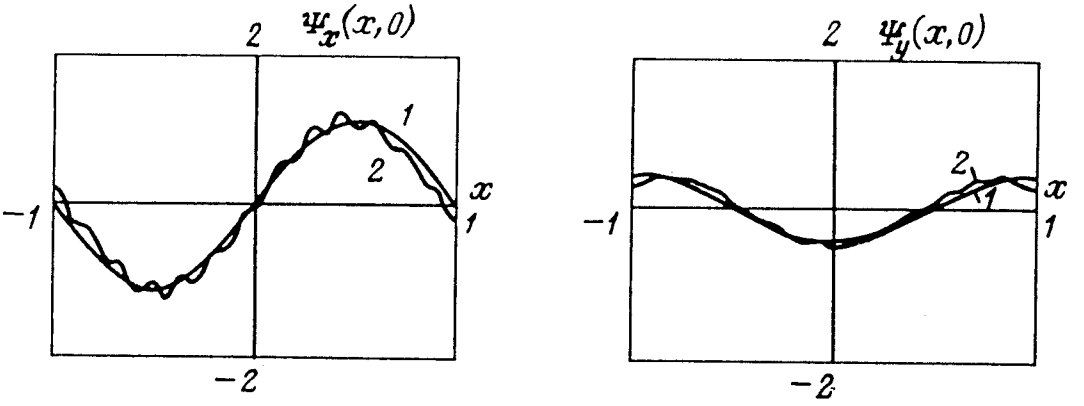

Fig. 6

theory (curves *1*) and by the exact theory (curves 2) are in quite good agreement, which allows us to conclude that the approximate theory suggested in [1] provides high accuracy in predicting natural shapes as well. This statement is valid for the overwhelming majority of natural shapes. Nevertheless, in exceptional cases, the difference in natural shapes predicted by the exact and approximate theories can be arbitrarily large. It should be emphasized that such cases are encountered rather rarely: among all natural shapes found in the course of the present investigation (10 natural shapes were calculated for each of the eight types of boundary conditions), the exact and approximate theories were established to disagree only in one case—in predicting the 7th natural shape for the case of the weakened clamping conditions (1.8)

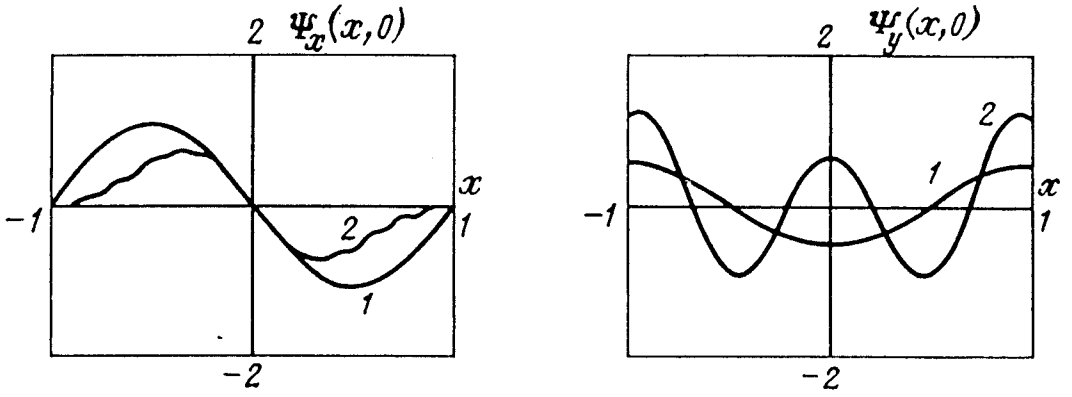

Fig. 7

at the sides $x = \pm a$ (see the graphs of Ψ_x and Ψ_y versus x in Fig. 7). Although the exact and approximate theories considerably disagree in predicting natural shapes extremely rarely, this phenomenon, apparently, is not accidental and, therefore, deserves a detailed discussion.

Below we present the results for the 6th and 7th natural shapes corresponding to the Reissner theory (the functions are marked by superscript R) and those corresponding to the approximate theory (no superscripts). The calculations were made for $h = 0.1$ m, assuming that conditions (1.8) were satisfied at $x = \pm a$.

For the sixth (shear) shape, we have

$$\omega^{\mathrm{R}} = 104918.313, \quad \Phi^{\mathrm{R}}(x,y) = 0, \quad F^{\mathrm{R}}(x,y) = 0.190\sin(6.28\,x)\sin(1.57\,y),$$
$$\omega = 104918.320, \quad \Phi(x,y) = 0, \quad F(x,y) = 0.190\sin(6.28\,x)\sin(1.57\,y),$$

and for the seventh (bending) shape,

$$\omega^{\mathrm{R}} = 105093.930, \quad F^{\mathrm{R}}(x,y) = -0.147\sin(6.56\,x)\sin(1.57\,y),$$
$$\Phi^{\mathrm{R}}(x,y) = [0.186\cos(3.26\,x) + 0.0005\cos(40.39\,x)]\cos(1.57\,y),$$
$$\omega = 104980.414, \quad F(x,y) = 0, \quad \Phi(x,y) = 0.350\cos(3.14\,x)\cos(1.57\,y).$$

When discussing what cased the low accuracy in calculating the 7th vibrational shape, one should pay attention to the following two points.

The error $\delta = 0.108\%$ of calculation of the 7th natural frequency by the approximate theory is not too large in the sense that there are frequencies for which the approximate theory leads to the same errors, but the corresponding natural shapes are predicted quite well. Therefore, we can state with certainty that the cause of the so significant difference of the exact 7th shape from the approximate one bears no relation to the accuracy of the prediction of the natural frequency.

The 6th and 7th natural frequencies are very close to each other and, which is more important, the values of the corresponding values λ_1^{R} and δ^{R} are also rather close. The latter means that the functions $\Phi_n^{\mathrm{R}} = C_{1n}\cos(\lambda_{1n}^{\mathrm{R}}x)\cos(\mu_n y)$ and $F_n^{\mathrm{R}} = C_{3n}\sin(\delta^{\mathrm{R}}x)\sin(\mu_n y)$ for the 7th vibrational shape differ from the respective functions for the 6th vibrational shape merely in the values of C_1 and C_3: in the case of the 6th (shear) shape, C_1 must be small, whereas in the case of the 7th (bending) shape, C_3 must be small. Based on the above facts, we can state with high degree of certainty that the cause of the bad prediction of the 7th vibrational shape is a combination of such factors as the closeness of the 6th and 7th natural frequencies and the likeness of the respective natural shapes. However, it remains unclear what actually happens, whether the approximate theory fails or the accumulation of errors in computations by the exact Reissner theory leads to a wrong prediction of the natural shape.

5. CONCLUSION

The approximate theory of high-frequency free vibrations suggested in [1] is convenient from the viewpoint of the numerical implementation, since this theory does not contain functions rapidly varying in the spatial coordinates. The approximate theory allows one to calculate natural frequencies and the respective vibrational shapes with high

accuracy, including those for thick plates. As the frequency number in a spectrum increases, the accuracy of the theory decreases insignificantly.

Nevertheless, the approximate theory suggested in [1] does not removes all difficulties related to the problem of high-frequency free vibrations.

First, this theory does not allow one to find the natural frequencies of the low-frequency spectrum which are close to frequencies of high-frequency spectra.

Second, the question related to possible loss of accuracy of computation of natural shapes in the case where a shear frequency turns out to be very close to a bending frequency is still a challenge.

ACKNOWLEDGMENTS

The author would like to thank P. A. Zhilin and Yu. G. Ispolov for useful discussion of the problem and valuable remarks.

REFERENCES

[1] E. A. Ivanova, "Approximate Hamiltonian functionals in problems on low-frequency and high-frequency free vibrations of Reissner's plate," Izv. AN. MTT [Mechanics of Solids], No. 4, pp. 181–190, 1995.

[2] Vibration in Engineering. Volume 1 [in Russian], Mashinostroenie, Moscow, 1978.

St. Petersburg